



# Study on the natural radioactivity level of stone coal-bearing strata in East China

Naizheng Xu<sup>1</sup> · Xinxiang Wei<sup>2</sup> · Fuxiang Kuang<sup>1</sup> · Linxi Zhang<sup>2</sup> · Hongying Liu<sup>1</sup>

Received: 19 July 2018 / Accepted: 21 October 2018 / Published online: 26 October 2018  
© Springer-Verlag GmbH Germany, part of Springer Nature 2018

## Abstract

Based on  $\gamma$ -radiation dose rate and radon concentration measurements and  $^{238}\text{U}$ ,  $^{232}\text{Th}$ ,  $^{226}\text{Ra}$ , and  $^{40}\text{K}$  radionuclide testing, this study identifies the radioactive anomalies of stone coal-bearing strata in East China and evaluates the natural radioactivity levels in the air, solid, water and plant media in the typical area of the regional stone coal-bearing layers. The stone coal-bearing strata in East China occur in the lower Cambrian system along the margin of the Yangtze block; additionally, the radioactive anomaly area is sporadically distributed in the stone coal-bearing layers. The background values of  $^{238}\text{U}$ ,  $^{232}\text{Th}$ ,  $^{226}\text{Ra}$ , and  $^{40}\text{K}$  are higher in the stone coal-bearing areas, and the spatial distribution of these natural radionuclides shows significant variability.  $^{238}\text{U}$  and  $^{226}\text{Ra}$  clearly accumulate in the coal, coal gangue and soil and are the main sources of the environmental radiation in coal mines. The  $\gamma$ -radiation shows a higher background value in the stone coal-bearing area, and this radioactive pollution cannot be ignored. Typically, the effective dose of  $\gamma$ -radiation exceeds the limit value of 5 mSv/a, and the total  $\alpha$  and total  $\beta$  concentrations of the groundwater are 10–30 times the limit value at some points. The residents near the mining area are subjected to a higher radiation dose, and the groundwater, building materials, and plants have been contaminated by the radioactive pollution sporadically through time. It is necessary to strengthen the monitoring work of radioactive environments and to take appropriate control measures.

**Keywords** Stone coal-bearing strata · Natural radioactivity · Radiation dose · East China

## Introduction

Natural radiation mainly originates from the decay of natural radionuclides, with a small part from the radiation of cosmic rays. The decay of the radionuclides  $^{238}\text{U}$ ,  $^{232}\text{Th}$ ,  $^{226}\text{Ra}$ ,  $^{40}\text{K}$ , etc., generates decay daughters and releases  $\alpha$ ,  $\beta$  and  $\gamma$ -rays at the same time. During the exploitation and utilization of radionuclide-containing coal mines, the natural radionuclides will be released into the air, soil and water media, thereby increasing the concentration of the natural radionuclides originally present in the environment and causing radioactive contamination (Chałupnik et al. 2017; Galhardi et al. 2017; Jiang 2007; Křibek et al. 2018; Skoko et al. 2017; Wufuer et al. 2018; Ye et al. 2004a). At present,

studies of the radioactive environment mainly focus on the survey and analysis of coal (coal gangue) (Huang and Tan 2002; Wang et al. 2017a, b; Xiong et al. 2007), soil (Galhardi et al. 2017; Skoko et al. 2017; Yue et al. 2011), biology (Galhardi et al. 2017; Skoko et al. 2017; Wufuer et al. 2018; Zhang et al. 2011), and water bodies (Chałupnik et al. 2017; Křibek et al. 2018).

The special study on the radioactivity of coal-bearing strata in China was initiated in the 1960s. The nationwide survey of the environmental natural radioactivity level (Luo et al. 1995) conducted in the 1980s and the national database of the radionuclide content in coal mines (Liu et al. 2006, 2007) established in 2000 have provided reference data and an evaluation basis for the survey and research of the radioactive environment. According to the implemented survey and evaluation of the radioactivity levels of the natural radionuclides in the coal-bearing strata (Huang and Tan 2002; Jiang 2007; Liu et al. 2006, 2007; Lu 2003; Wang et al. 2017a, b; Ye et al. 2004a, b), radioactive anomalies exist in the coal strata in East China, and natural radionuclides, including  $^{238}\text{U}$ ,  $^{232}\text{Th}$ ,

✉ Naizheng Xu  
xzzz100@sina.com

<sup>1</sup> Nanjing Center, China Geological Survey, Nanjing 210016, China

<sup>2</sup> Jiangxi Nuclear Industry Geological Bureau Testing Center, Nanchang 330002, China

$^{226}\text{Ra}$  and  $^{40}\text{K}$ , were found in the coal. Their content was clearly higher than that in the common coal and soil, and the anomalous distribution showed an obvious spatial variability. The basic grids for the radioactivity survey of the coal-bearing strata in East China that were carried out were  $25 \times 25$  km and  $50 \times 50$  km (Luo et al. 1995; Wang et al. 2017a, b; WGSR 1992), and the survey was limited to the surface layer. The survey research data was fragmentary and rough, with a low survey and evaluation accuracy. Since the 1990s, the coal mines in eastern China have undergone large-scale exploitation, shutdown, and reclamation. There have been no detailed systematic surveys and evaluations of the radioactive environmental quality after exploitation in the mining area. Based on the technical assessment method of the radioactive geological environment, this study will identify the radioactive anomalous strata in the stone coal-bearing strata of East China and assesses the status quo of the radioactive environment of the main coal layers, with a focus on providing basic data for the monitoring and treatment of the regional radiation risk.

## Outline of the study area

### Geography and geology

East China is located on the eastern coast of China, adjoining Shandong in the north, neighboring Henan, Hubei and Hunan in the west, abutting Guangdong in the south, and is close to the Yellow Sea and the East China Sea to the east. Its geographical coordinates are  $23^{\circ}30' - 35^{\circ}08' \text{N}$ ,  $113^{\circ}34' - 123^{\circ}40' \text{E}$ ; it includes 5 provinces and 1 municipality, namely, Zhejiang, Jiangsu, Fujian, Jiangxi, Anhui and Shanghai, covering a total area of  $638,600 \text{ km}^2$ . The area is vast and the climate is changeable. The Huai River–North Jiangsu Main Irrigation Channel is the dividing line between the warm temperate zone and the subtropical zone. From the north to the south, the climate transitions from a semihumid monsoon climate of a warm temperate zone to the subtropical–tropical monsoon climate zone. East China lies on the southern margin of the Eurasian Block, near the western Pacific Ocean. It is a typical tectonic zone where the Eurasia Block proliferates to the east and south, followed by the continental breakup-disintegration of the continental plates (Zhang et al. 2015). The tectonic structure of East China spans three tectonic units, i.e., the North China block, Yangtze block, and the Southeast coastal orogenic belt. The area north of the Huai River belongs to the North China block; most of the Jiangsu Province, Shanghai and northern Zhejiang Province belong to the Yangtze block, and

the southern Zhejiang and Fujian Province belong to the Southeast coastal orogenic belt (Fig. 1).

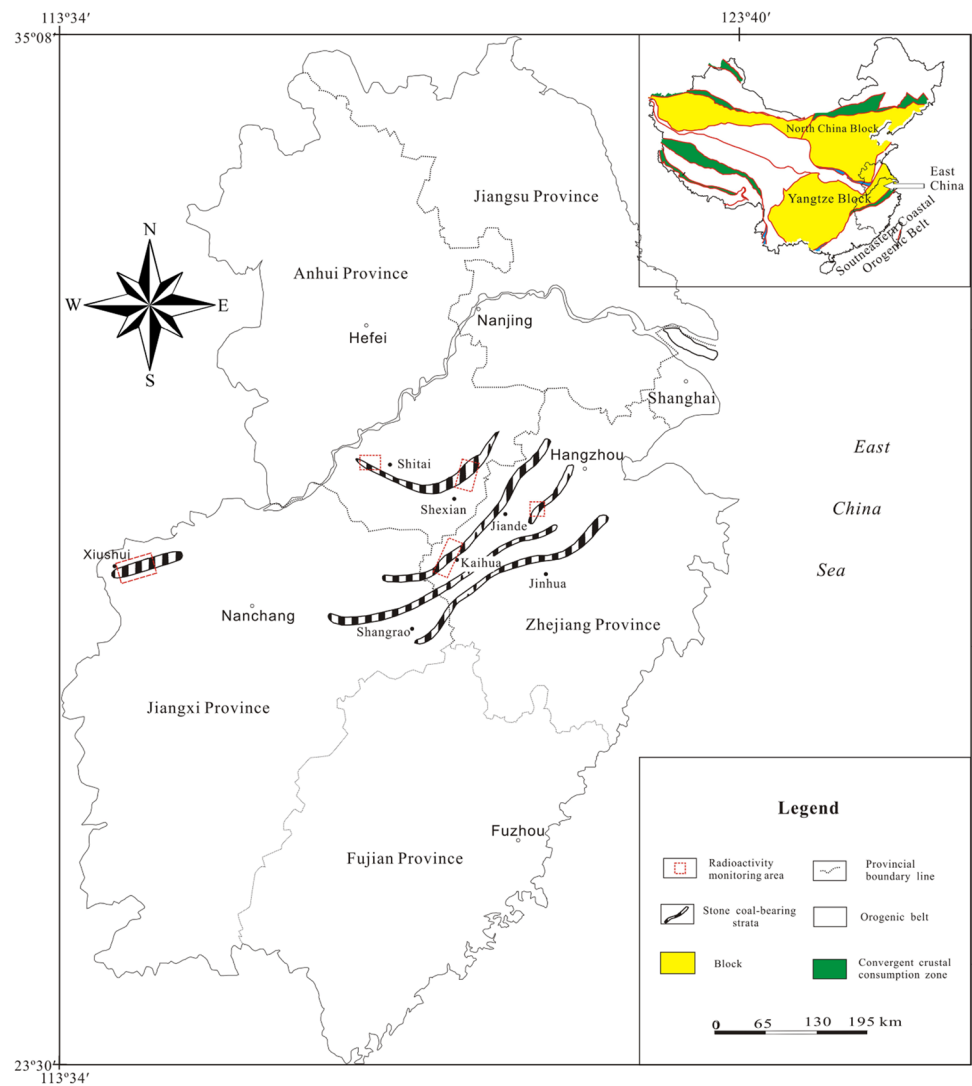
### Temporal and spatial distribution of the stone coal-bearing strata

The occurrence of a coal seam is controlled by the geotectonic evolution, sedimentation and other factors. The stone coal-bearing sedimentary formations in East China mainly occur in the Carboniferous, Permian, Triassic, and Jurassic strata. The radioactive coal mines in East China mainly contain coal that formed in the lower Cambrian strata and that was deposited in a deepwater reduction environment. The Hetang formation ( $\epsilon_1 h$ ) is the main stratum of coal in the region. Its lithological characteristics are mainly a set of dark gray and gray black carbonaceous silty mudstone. The stone coal-bearing strata in East China is spatially located on the margin of the Yangtze block, and distributed in a band shape to the NE mainly in the hilly areas of Zhejiang, Jiangxi and Anhui Province (Ye et al. 2004a, b; Wang et al. 2017a, b) (Fig. 1). The coal resources of Jiangxi are mainly distributed in Jiujiang, Xiushui, Shangrao, and Yushan; those of Anhui are mainly in the mountain areas of Huangshan and Xuancheng, and those of Zhejiang are mainly in Quzhou, Shaoxing, and Hangzhou. The stone coal-bearing strata has undergone the superimposition of multiple tectonic movements of the Caledonian, Indosinian, Yanshanian and Himalayan periods, and formed a series of linear folds and brittle fractures under different mechanisms, chiefly in the NE direction, followed by the NNE and NW directions. The stone coal is shallowly buried, and its thickness varies. Stone coal is a kind of inferior anthracite with low carbon content and low calorific value along with higher degree of coalification and ash contents. Most of it is exploited conveniently by open-pit mining.

### Measurements and methods

According to the past radioactivity survey records, this study focused on the survey and evaluation of the radioactive geological environment in the distribution area of the Cambrian black rock series. A total of 248 measuring points of the  $\gamma$ -radiation dose rates and 52 radon concentration monitoring points were arranged, with a monitoring area of  $220 \text{ km}^2$ . A total of 236 samples were taken and analyzed in the mining area, including coal, coal cinder, coal gangue, soil, sediments, carbonated lime brick, surface water, groundwater and plants. The coal strata in Xiushui of Jiangxi Province, Shexian and Shitai of Anhui Province, and the Kaihua and Jiande regions of Zhejiang Province are extensively exposed, and the distribution of the stone coal occurrences is concentrated. They are the key mining areas for this survey research. Measurement of

**Fig. 1** Distribution of the stone coal-bearing strata and radioactivity monitoring areas in East China



the  $\gamma$ -radiation dose rate and radon concentration was conducted during the field monitoring. The radioactivity survey and evaluation were based on the Norm for the Specification for Measurement of Dose Rate of Ambient Ground Gamma Radiation (SEPA 1993) and the Evaluation Requirements for the Environmental Impact of Uranium Geological Radiation Environment (CNIC 1995). Regarding the  $\gamma$ -radiation dose rate, the monitoring points were arranged using the grid method, with an accuracy of 1 km  $\times$  0.5 km or 1 km  $\times$  1 km, and measured with an environmental X $\cdot$  $\gamma$ -dose rate meter (Thermo Fisher, FHT40NBR, USA). The outdoor air radon concentration was measured at the coal occurrence outcropping area with a high-sensitivity environmental radon monitor (Durridge, RAD7, USA). The sampling points were set by using an approximate grid method, and the sampling was carried out according to the Specification for Multi-Purpose Regional Geochemical Survey (1:250,000). The sample processing test was conducted according to the EJ/T 751-2014 Specification for Testing Quality Assurance of Radioactive

Geological Laboratories (China Geological and Survey 2014) and other standards. The samples of coal, coal cinder, coal gangue, soil, sediments, carbonated lime brick and plants were analyzed for the specific activity of the radionuclides  $^{238}\text{U}$ ,  $^{232}\text{Th}$ ,  $^{226}\text{Ra}$  and  $^{40}\text{K}$ , and the analysis items of the water samples were  $^{238}\text{U}$ ,  $^{232}\text{Th}$ ,  $^{226}\text{Ra}$ ,  $^{40}\text{K}$ , total  $\alpha$  and total  $\beta$ .

The measuring instrument and methods for laboratory analyses and field monitoring in this study are provided in Table 1.

For the statistical analysis, SPSS19.0 was used as a platform for the descriptive statistical analysis, correlation analysis, and regression analysis. The thematic maps were produced by using Mapgis 6.7 and Surfer 12.

**Table 1** Measurement techniques for laboratory analyses and radioactivity survey of the stone coal-bearing strata in East China

Measuring item	Instrument	Instrument model	Instrument manufacturer	Sensitivity	Accuracy
Water samples					
$^{238}\text{U}$	Laser fluorescence uranium meter	HD-3025	Beijing hedi sci-tech development Co., Ltd, China	0.03 ng/mL	$\leq \pm 8\%$
$^{232}\text{Th}$	UV-Vis spectrophotometer	UV-1200	Macy instrument, China	0.001 ng/mL	$\leq \pm 5\%$
$^{226}\text{Ra}$	Radon and thorium analyzer	FD125	Beijing hedi sci-tech development Co., Ltd, China	1.27 mBq/L	$\leq \pm 10\%$
$^{40}\text{K}$	Atomic absorption spectrophotometer	CAAm-2001	Beijing HTH instrument Co., Ltd, China	2.86 mBq/L	$\leq \pm 5\%$
Total $\alpha$ , total $\beta$	Low background $\alpha$ , $\beta$ measuring instrument	HD-2011	Beijing hedi sci-tech development Co., Ltd, China	$\alpha$ : 0.005 Bq/L ; $\beta$ : 0.025 Bq/L	$\alpha$ : $\leq \pm 2\%$ $\beta$ : $\leq \pm 3\%$
Solid and plant samples					
$^{238}\text{U}$ , $^{232}\text{Th}$ , $^{226}\text{Ra}$ , $^{40}\text{K}$	HP Ge $\gamma$ -spectrometer	ADCAM-100	ORTEC, USA	$^{238}\text{U}$ : 0.9 Bq/kg $^{232}\text{Th}$ : 0.3 Bq/kg $^{226}\text{Ra}$ : 0.9 Bq/kg $^{40}\text{K}$ : 0.3 Bq/kg	$^{238}\text{U}$ : $\leq \pm 3.3\%$ $^{232}\text{Th}$ : $\leq \pm 15.8\%$ $^{226}\text{Ra}$ : $\leq \pm 4.4\%$ $^{40}\text{K}$ : $\leq \pm 3.8\%$
Radioactivity survey					
$\gamma$ -radiation dose rate	X $\gamma$ -dose rate meter	FHT40NBR	Thermo Fisher, USA	2000s-1/ $\mu\text{Sv/h}$	$\leq \pm 5\%$
Radon concentration	Environmental radon monitor	RAD7	Durridge, USA	0.5 CPM/pCi/L	$\leq \pm 5\%$

## Results and discussion

### Radionuclide concentration in solid media

In this study, 6 types of solid medium samples, including coal, coal cinder, coal gangue, soil, sediments and carbonated lime bricks were collected, totaling 146 samples (Table 2). The mean values of  $^{238}\text{U}$ ,  $^{232}\text{Th}$ ,  $^{226}\text{Ra}$  and  $^{40}\text{K}$  were  $669.1 \pm 1501.6$ ,  $34.8 \pm 19.1$ ,  $488.7 \pm 295.6$  and  $746.6 \pm 494.9$  Bq/kg, respectively. The content ranges of the 4 radionuclides were 64.7–6071.0, 10.3–78.4, 76.3–924.8 and 131.2–1676.0 Bq/kg, and their coefficients of variation were 2.24, 0.55, 0.60, and 0.66, respectively, showing a significant spatial variability in the radionuclide distribution and reflecting a geochemical background with significant differences in the coal mining area. The mean contents of  $^{238}\text{U}$ ,  $^{226}\text{Ra}$  and  $^{40}\text{K}$  were 5–8 times the Chinese national coal average and that of  $^{232}\text{Th}$  was slightly lower than the national measurement (Liu et al. 2007). This shows that the coal in the study area has a strong enrichment effect on the radionuclides of  $^{238}\text{U}$ ,  $^{226}\text{Ra}$  and  $^{40}\text{K}$ .

The mean values of  $^{238}\text{U}$ ,  $^{232}\text{Th}$ ,  $^{226}\text{Ra}$  and  $^{40}\text{K}$  in the coal gangue were  $330.2 \pm 367.6$ ,  $34.9 \pm 21.1$ ,  $329.2 \pm 317.6$ , and  $853.1 \pm 697.5$  Bq/kg, respectively. The content ranges of the 4 radionuclides were 43.5–1572.0, 8.3–83.2, 44.5–1197.0, and 157.7–2242.0 Bq/kg, and their coefficients of variation were 1.11, 0.60, 0.96, and 0.82, respectively, also showing a significant spatial variability in the radionuclide distribution. The mean contents of  $^{238}\text{U}$ ,  $^{226}\text{Ra}$  and  $^{40}\text{K}$  were 2–6 times the Chinese national coal gangue average and that of  $^{232}\text{Th}$  was lower than the national measurement (Liu et al. 2007). The

radionuclide contents of  $^{238}\text{U}$ ,  $^{232}\text{Th}$ ,  $^{226}\text{Ra}$  and  $^{40}\text{K}$  found in the investigated areas were much higher than the contents reported from stone coals from Australia, Russia (Dai et al. 2015). This also showed the enrichment effect of the coal gangue on the radionuclides of  $^{238}\text{U}$ ,  $^{226}\text{Ra}$  and  $^{40}\text{K}$ .

The radionuclide contents of  $^{238}\text{U}$ ,  $^{232}\text{Th}$ ,  $^{226}\text{Ra}$  and  $^{40}\text{K}$  in the soil were  $89.5 \pm 105.0$ ,  $48.5 \pm 12.7$ ,  $94.6 \pm 107.5$  and  $555.2 \pm 200.2$  Bq/kg, respectively. The content ranges of the 4 radionuclides were 21.9–689.5, 18.5–87.7, 21.9–655.2 and 240.4–1291.0 Bq/kg, and their coefficients of variation were 1.17, 0.26, 1.14 and 0.36, respectively, also showing a significant spatial variability in the radionuclide distribution.  $^{238}\text{U}$  and  $^{226}\text{Ra}$  were 2–3 times the national soil measurement value, and  $^{232}\text{Th}$  was close to the national soil measurement value (WGSR 1992), indicating the high background radiation level of the radionuclides  $^{238}\text{U}$  and  $^{226}\text{Ra}$  in the soil of the coal mining area.

The radionuclide contents of  $^{238}\text{U}$ ,  $^{232}\text{Th}$ ,  $^{226}\text{Ra}$  and  $^{40}\text{K}$  in the sediment were  $70.4 \pm 65.5$ ,  $40.0 \pm 10.1$ ,  $58.7 \pm 52.7$ , and  $728.5 \pm 180.3$  Bq/kg, respectively, which were relatively low. The radionuclide contents of  $^{238}\text{U}$ ,  $^{232}\text{Th}$ ,  $^{226}\text{Ra}$  and  $^{40}\text{K}$  in the coal cinder were  $196.7 \pm 115.4$ ,  $44.8 \pm 14.4$ ,  $258.4 \pm 102.3$  and  $1038.9 \pm 576.9$  Bq/kg, respectively. The enrichment effect of the coal on the radionuclides after combustion was not obvious. The coal cinder and coal gangue were the common building materials in the production of the carbonated lime brick in the coal mining area. The radionuclide contents of  $^{238}\text{U}$ ,  $^{232}\text{Th}$ ,  $^{226}\text{Ra}$  and  $^{40}\text{K}$  in the carbonated lime brick detected in this study were, respectively,  $368.3 \pm 242.0$ ,  $16.2 \pm 7.7$ ,  $234.3 \pm 293.8$  and  $184.5 \pm 160.3$  Bq/kg, equivalent to those in the coal gangue

**Table 2** Average contents of the natural radionuclides in the solid media of the stone coal-bearing strata in East China

Stone coal occurrence	Radioactive medium	Sample quantity (pcs)	$^{238}\text{U}$ (Bq/kg)	$^{232}\text{Th}$ (Bq/kg)	$^{226}\text{Ra}$ (Bq/kg)	$^{40}\text{K}$ (Bq/kg)
Shexian of Anhui	Coal	4	1865.1 ± 2806.2	24.2 ± 8.2	640.1 ± 284.8	440.2 ± 260.3
	Coal gangue	8	389.9 ± 196.6	33.1 ± 22.0	337.6 ± 173.2	470.5 ± 258.4
	Soil	53	85.5 ± 97.1	44.7 ± 10.4	89.9 ± 100.4	488.5 ± 132.4
	Sediments	4	60.1 ± 58.0	39.7 ± 8.4	61.0 ± 72.3	675.0 ± 246.8
	Carbonated lime brick	2	340.9 ± 335.5	20.6 ± 0.8	331.5 ± 340.4	276.5 ± 25.5
Shitai of Anhui	Coal	1	197.0	17.0	489.5	494.1
	Coal gangue	2	269.6 ± 205.2	12.7 ± 6.1	699.3 ± 703.9	325.4 ± 201.4
	Soil	8	64.3 ± 38.4	43.3 ± 7.4	90.7 ± 69.5	515.2 ± 90.1
	Sediments	1	77.8	28.0	61.5	591.4
Xiushui of Jiangxi	Coal	6	257.7 ± 141.1	37.0 ± 25.5	585.1 ± 308.5	559.2 ± 382.2
	Coal cinder	4	292.7 ± 123.7	42.5 ± 30.6	716.6 ± 285.0	694.6 ± 444.9
	Soil	6	134.0 ± 72.8	60.3 ± 23.2	154.9 ± 104.9	466.0 ± 102.3
	Stream sediments	3	28.4 ± 13.9	33.5 ± 12.4	28.5 ± 6.3	756.7 ± 245.7
	Carbonated lime brick	1	423.1	39.8	494.9	516.3
Kaihua of Zhejiang	Coal	3	163.7 ± 66.3	47.8 ± 12.3	175.5 ± 53.8	1478.3 ± 190.0
	Coal cinder	3	169.1 ± 39.3	43.4 ± 14.0	188.9 ± 15.5	1387.0 ± 104.9
	Coal gangue	4	508.4 ± 715.1	42.6 ± 25.3	363.1 ± 409.6	1106.4 ± 609.0
	Soil	12	48.3 ± 19.3	52.6 ± 7.7	52.0 ± 16.0	624.2 ± 123.1
	Sediments	2	48.8 ± 8.9	44.1 ± 10.6	30.9 ± 10.8	743.3 ± 88.0
Jiande of Zhejiang	Coal	1	342.5	42.6	243.9	1154.0
	Coal gangue	4	62.8 ± 22.4	41.8 ± 16.1	93.5 ± 40.3	1628.8 ± 867.8
	Soil	11	85.0 ± 88.9	62.4 ± 7.2	84.8 ± 92.9	919.2 ± 247.9
	Sediments	3	138.2 ± 101.1	48.3 ± 6.5	103.3 ± 60.0	807.6 ± 116.8
Nationwide	Coal <sup>a</sup>	1014	79.5 ± 45.0	40.3 ± 34.0	73.9 ± 53.0	152.4 ± 2121.0
	Coal gangue <sup>a</sup>	879	79.8 ± 34.0	64.5 ± 38.0	59.7 ± 44.0	506.3 ± 477.0
	Soil <sup>b</sup>	7777	39.5 ± 34.4	49.1 ± 27.6	36.5 ± 22.0	580.0 ± 202.0

<sup>a</sup>Liu et al. (2007)<sup>b</sup>WGSR (1992)

and coal cinder overall. The detected  $^{226}\text{Ra}$  content in the carbonated lime brick exceeded the national standard limit ( $\leq 200$  Bq/kg) (Lu 2003), and it should not be used for habitation building constructions.

The specific higher radiation levels were associated with igneous rocks, such as granite, which had relatively high content of uranium. Uranium abundance of continental crust in East China was 3.7 ppm, which was 1.37 times of continental crust, especially, uranium abundance in Lower Sinian to lower Cambrian strata ranged from 20 to 100 ppm. Thus, higher radiation levels originated from high radionuclides.

After the analysis of the distribution of the radionuclides  $^{238}\text{U}$ ,  $^{232}\text{Th}$ ,  $^{226}\text{Ra}$  and  $^{40}\text{K}$  in each solid medium, it was found that  $^{238}\text{U}$  and  $^{226}\text{Ra}$  were significantly enriched in the coal and coal gangue, and their mean contents were 2–8 times those of the other media.  $^{226}\text{Ra}$  was the decay daughter of  $^{238}\text{U}$ , and the content of the  $^{226}\text{Ra}$  was controlled by the  $^{238}\text{U}$  content. Because the coal was rich in organic matter, it had a strong adsorption effect on  $^{238}\text{U}$  and exhibited a

high content of  $^{238}\text{U}$  and  $^{226}\text{Ra}$  (Huang and Tan 2002; Ishak and Dunlop 1985; Xiong et al. 2007). As the coal and coal gangue of the stone coal-bearing strata were enriched with  $^{238}\text{U}$ ,  $^{226}\text{Ra}$  and other radionuclides, the exploitation and utilization of the coal would result in the accumulation of the associated radionuclides  $^{238}\text{U}$  and  $^{226}\text{Ra}$  in the soil, as well as the appearance of the high background radiation level of the radionuclides  $^{238}\text{U}$  and  $^{226}\text{Ra}$  in the local soil of the mining area.

### Radionuclide concentration in water bodies

Samples of the surface water and groundwater were collected in this study. The surface water was mainly taken from the rivers and lakes in the mining area, while the groundwater was taken from the shallow wells and pits in the mining area. A total of 53 surface water samples and 25 groundwater samples were collected and tested (Table 3). The spatial distribution of the radionuclides  $^{238}\text{U}$ ,  $^{232}\text{Th}$ ,  $^{226}\text{Ra}$  and  $^{40}\text{K}$

**Table 3** Average concentration of the natural radionuclides in the water media of the stone coal-bearing strata in East China

Stone coal occurrence	Radioactive medium	Sample quantity (pcs)	$^{238}\text{U}$ (Bq/L)	$^{232}\text{Th}$ (Bq/L)	$^{226}\text{Ra}$ (Bq/L)	$^{40}\text{K}$ (Bq/L)	Total $\alpha$ (Bq/L)	Total $\beta$ (Bq/L)
Shexian of Anhui	Surface water in mining area	17	0.71	0	0.12	0.17	0.80	0.81
	Groundwater in mining area	7	0.01	0	0.01	0.03	0.06	0.06
Shitai of Anhui	Surface water in mining area	18	0	0	0.05	0.02	0.23	0.10
	Groundwater in mining area	6	0	0	0	0.15	0.02	0.18
Xiushui of Jiangxi	Surface water in mining area	6	0.40	0	0.01	0.10	0.30	0.30
	Groundwater in mining area	5	0.20	0	0.01	0.20	0.40	0.40
Kaihua of Zhejiang	Surface water in mining area	7	0	0	0	0.05	0.02	0.05
	Groundwater in mining area	3	7.15	0.10	0.07	0.08	7.90	8.83
Jiande of Zhejiang	Surface water in mining area	5	0.56	0	0.01	0.14	0.64	0.53
	Groundwater in mining area	4	2.44	0.05	0.02	0.14	2.52	3.59

and total  $\alpha$  and total  $\beta$  were significantly different. The radioactivity of  $^{238}\text{U}$ ,  $^{226}\text{Ra}$ ,  $^{40}\text{K}$ , total  $\alpha$  and total  $\beta$  in the surface water were  $0.33 \pm 3.08$ ,  $0.04 \pm 0.05$ ,  $0.10 \pm 0.06$ ,  $0.40 \pm 0.32$  and  $0.36 \pm 0.32$  Bq/kg, respectively. The concentration of  $^{232}\text{Th}$  in the surface water bodies of each mining area was very low. Compared with the radioactivity of the surface water in the nationwide survey of the environmental natural radioactivity level (Luo et al. 1995), this study showed that the radionuclide content in the surface water was generally at a normal level. The radioactivity of  $^{238}\text{U}$ ,  $^{232}\text{Th}$ ,  $^{226}\text{Ra}$ ,  $^{40}\text{K}$ , total  $\alpha$  and total  $\beta$  in the groundwater were  $1.96 \pm 3.08$ ,  $0.03 \pm 0.04$ ,  $0.02 \pm 0.03$ ,  $0.12 \pm 0.07$ ,  $2.18 \pm 3.36$  and  $2.61 \pm 3.77$  Bq/kg, respectively. The mean concentrations of  $^{238}\text{U}$ , total  $\alpha$  and total  $\beta$  in groundwater was 5–7 times the mean value of the surface water. The total  $\alpha$  and total  $\beta$  exceeded the limits of the Guidelines for Drinking-Water Quality of 0.5 Bq/L and 1 Bq/L (WHO 2011), and the total  $\alpha$  and total  $\beta$  of some stone coal occurrences were 10–30 times the limits. The groundwater with high  $^{238}\text{U}$ , total  $\alpha$  and total  $\beta$  had a low pH (<5). Under acidic conditions, the radionuclides U and Ra showed a strong geochemical activity.

### Radionuclide concentration in plants

The plant samples taken in this study were representative indicator plants widely distributed in the investigated mining area, such as corn, pine, reed, tea and sweet potato. These plants grow in the soil originated from the pedogenesis of

stone coal-bearing strata. Among them, the corn samples were taken from roots, stalk, and seeds for the radionuclide analysis. For each sample a number of at least three individuals were sampled. A total of 12 samples of plant tissues were collected and tested (Table 4). The radionuclide contents of  $^{238}\text{U}$ ,  $^{232}\text{Th}$ ,  $^{226}\text{Ra}$  and  $^{40}\text{K}$  in the plant tissues of were  $1.19 \pm 4.82$ ,  $0.18 \pm 0.31$ ,  $17.09 \pm 52.99$  and  $110.50 \pm 62.59$  Bq/kg, respectively. The content ranges of the 4 radionuclides were 0.01–5.67, 0–1.17, 0.11–185.30 and 24.26–283.40 Bq/kg, and their coefficients of variation were 4.05, 1.72, 3.10 and 0.57, respectively, showing a very significant spatial variability of the radionuclide distribution. The radionuclide content in the plant tissues is related to the radionuclide absorption and enrichment ability of the various plants, and it is also closely related to the background value of the natural radionuclides in the soil where the plants grow (Galhardi et al. 2017; Skoko et al. 2017). The soil in the coal mining area was characterized by a high content of  $^{238}\text{U}$  and  $^{226}\text{Ra}$ , and the content of  $^{238}\text{U}$  and  $^{226}\text{Ra}$  in the plant body was clearly increased. The radionuclide content in the plant body was positively correlated with the radionuclide content in soil. There were differences in the ability of the plant tissues to absorb and enrich a radionuclide. In this study, it was found that the contents of  $^{238}\text{U}$ ,  $^{232}\text{Th}$  and  $^{226}\text{Ra}$  in the roots, stalk and seeds of corn were significantly different, and their radioactivity decreased sharply in turn. The high background radiation levels of  $^{238}\text{U}$  and  $^{226}\text{Ra}$  in the soil of the mining area and the significant variation in the spatial

**Table 4** Average contents of the natural radionuclides in the plant samples

Stone coal occurrence	Plant species	Sample quantity (pcs)	<sup>238</sup> U (Bq/kg)	<sup>232</sup> Th (Bq/kg)	<sup>226</sup> Ra (Bq/kg)	<sup>40</sup> K (Bq/kg)
Shexian of Anhui	Corn root	3	3.67	1.11	3.34	130.20
	Corn stalk	3	1.65	0.34	2.47	283.10
	Corn seed	3	0.21	0.07	0.58	94.97
Shitai of Anhui	Tea	1	0.20	0.02	1.49	117.70
	Sweet potato	1	0.01	0.01	0.11	62.88
Xiushui of Jiangxi	Pine needle	1	0.06	0.06	0.51	24.26
	Cedar leaves	1	0.12	0.03	1.55	120.70
	Miscanthus floridulus	1	0.02	0.01	1.24	82.42
Kaihua of Zhejiang	Pine needle	1	2.16	0.25	3.97	105.70
	Reed	1	5.67	0.11	185.30	126.90
Jiande of Zhejiang	Cedar leaves	1	0.24	0.10	3.20	108.20
	Pine needle	1	0.22	0.02	1.35	69.00

distribution, as well as the differences in the radionuclide absorbing capacity of the plants, have determined the highly significant spatial variability of the radionuclide distribution in the plant body. In general, the specific activity of the radionuclides in the plant samples of the coal mining area in East China is relatively low, and there is no radiation risk with the normal planting and consumption in the local area. The current hyperaccumulator of <sup>226</sup>Ra was *Dicranopteris dichotoma* (Zhang et al. 2011). This study found that the content of <sup>226</sup>Ra in the plant samples (reed) in the Kaihua mining area of Zhejiang Province was as high as 185.3 Bq/kg, which was more than 100 times that of similar plants in the local area and was far more than the national limit of the radionuclide content in food. This shows an obvious <sup>226</sup>Ra enrichment feature, which may be interrelated with high contents of radioisotopes in soils. However, it is not representative enough due to limited data and is worth further survey and research.

### **$\gamma$ -external radiation intensity and effective dose**

Terrestrial space is a place where humans live. The environmental surface is always exposed to  $\gamma$ -radiation from the universe and natural radionuclides. Natural radiation is the main source of radiation exposure to humans, and the radiation produced by radon and its daughters is a major source of natural radiation (Pan and Liu 2011; Wang et al. 2014; UNSCEAR 2000). A normal dose of  $\gamma$ -radiation will not cause damage to human health, but high-intensity  $\gamma$ -radiation may cause damage to the human body. The damage that  $\gamma$ -rays impart on the human body depends on the radiation intensity and time. Generally, the effective dose limit is less than 1 mSv/a for public exposure (IAEA 2014). The effective radiation dose for the general public in the coal mining areas is mainly derived from the external radiation

and air inhalation pathways, and the proportion that originates from ingestion pathways is very small (less than 5%).

The estimating formula of the annual effective dose of the  $\gamma$ -external radiation provided in accordance with the Specification for Measurement of Dose Rate of Ambient Ground Gamma Radiation (GB/T 14583-93) (SEPA 1993) is:

$$H_r = D_r \times K \times t,$$

where  $H_r$  is the effective dose, in Sv/a;  $D_r$  is the  $\gamma$ -radiation air absorbed dose rate, in Gy/h;  $K$  is the dose conversion factor, which is 0.7 Sv/Gy; and  $t$  is the duration of stay for the general public in the area during the year, generally 8760 h.

The estimating formula of the internal radiation effective dose caused by the radon daughters inhaled by the general public in accordance with the Evaluation Requirements for the Environmental Impact of Uranium Geological Radiation Environment (EJ/T 977-1995) (CNIC 1995) is:

$$H_e = 0.5 \times \bar{X} \times g_E \times t,$$

where  $H_e$  is the effective dose, in Sv/a; 0.5 is the balance factor of radon and its daughters;  $\bar{X}$  is the average radon concentration, in Bq/m<sup>3</sup>;  $g_E$  is the dose conversion factor of the outdoor radon daughters inhaled by adults, which is  $1.7 \times 10^{-8}$  Sv/(Bq h/m<sup>3</sup>); and  $t$  is the duration of stay for the general public in the environment during the year, generally 8760 h.

In this study, the measurements of the  $\gamma$ -dose rate and outdoor radon concentration were conducted in the major coal areas in East China, and the annual effective dose of adult  $\gamma$ -external radiation, the annual effective dose of inhaled radon daughters and the total effective dose in the mining area were calculated (Table 5).

The average annual effective dose to the world population is approximately 2.4 mSv, and the total inhalation exposure and total external terrestrial radiation are 1.26 and 0.48 mSv

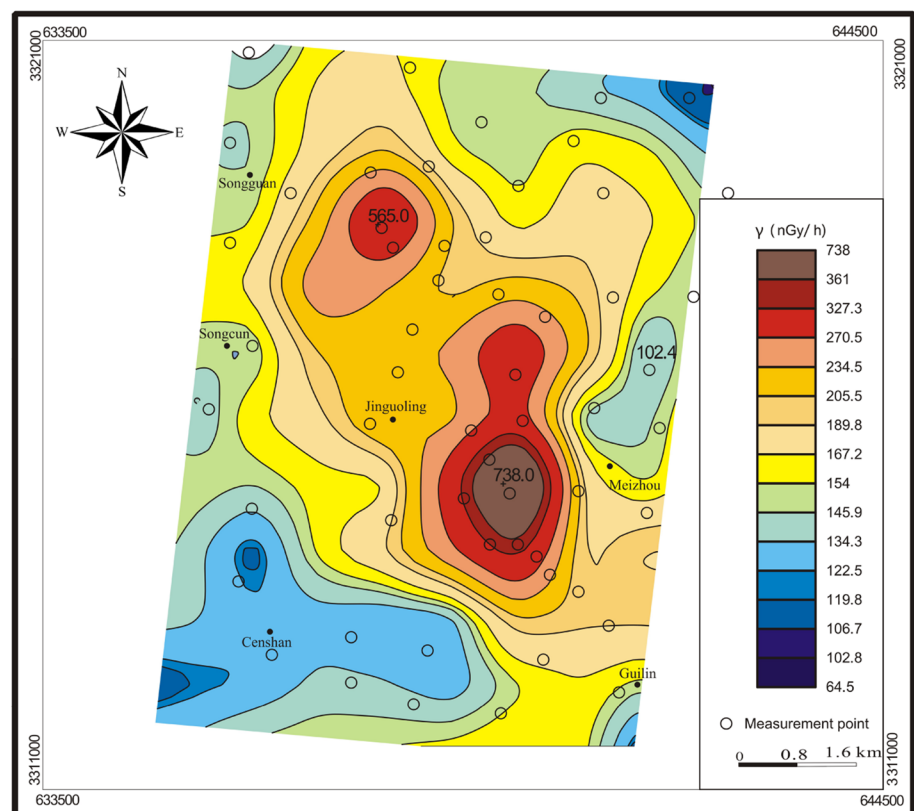
**Table 5** Terrestrial  $\gamma$ -external radiation intensity and the effective dose of the stone coal-bearing strata in East China

Mining area	Area (km <sup>2</sup> )	Ambient $\gamma$ -radiation dose rate (nGy/h)		Annual effective dose of $\gamma$ -external radiation (mSv/a)		Radon concentration (outdoor) (Bq/m <sup>3</sup> )		Annual effective dose of inhaled radon daughters (mSv/a)		Total effective dose (mSv/a)
		Mean	Range	Mean	Range	Mean	Range	Mean	Range	
Shexian of Anhui	69	183	52–725	1.04	0.24–4.37	47.10	33–81	3.51	2.45–6.05	4.55
Shitai of Anhui	16	218	71–956	1.26	0.36–5.78	62.00	33–98	4.60	2.45–7.30	5.86
Xiushui of Jiangxi	55	304	70–1179	1.86	0.43–7.23	12.23	3–31	0.91	0–2.31	2.77
Kaihua of Zhejiang	50	205	61–1514	1.26	0.37–9.28	20.70	12–28	1.54	0.89–2.08	2.80
Jiande of Zhejiang	30	210	55–571	1.29	0.34–3.50	20.20	0–59	1.50	0–4.39	2.79

(UNSCEAR 2000). In the main coal distribution zone in East China, the absorbed dose caused by  $\gamma$ -external radiation had exceeded 1 mSv/a, and the total effective dose had exceeded 2 mSv/a. It belongs to the overall high radiation value area. In some concentrated distribution areas of the coal mines, for example, in the mining areas of Shitai in Anhui, Kaihua in Zhejiang and Xiushui in Jiangxi, the effective doses caused by the  $\gamma$ -external radiation were all higher than the Chinese national warning limit of 5 mSv/a. The terrestrial radon concentrations in the mining areas of Shexian and Shitai in Anhui exceeded 30 Bq/m<sup>3</sup>, and the annual effective doses of the inhaled radon daughters exceeded

3 mSv/a. The doses of the  $\gamma$ -external radiation and inhaled radon daughters calculated in this study were close to the radioactivity monitoring results of the coal in 1991–1993 (Ye et al. 2004a). The total effective dose for the residents in the mining area was 2.77–5.86 mSv/a. Thus, the radioactive contamination in the coal mining area could not be ignored, and strict radioactivity monitoring should be implemented.

The isogram of the  $\gamma$ -radiation air absorbed dose rate in the Shexian work area in Anhui Province showed a clear distribution rule of “high in the middle and low in circumference”, forming an approximate NW–SE high-value field in an approximate elliptical shape (Fig. 2). Two prominent

**Fig. 2** Isogram of the  $\gamma$ -radiation dose rate in the stone coal-bearing strata in Shexian in Anhui Province



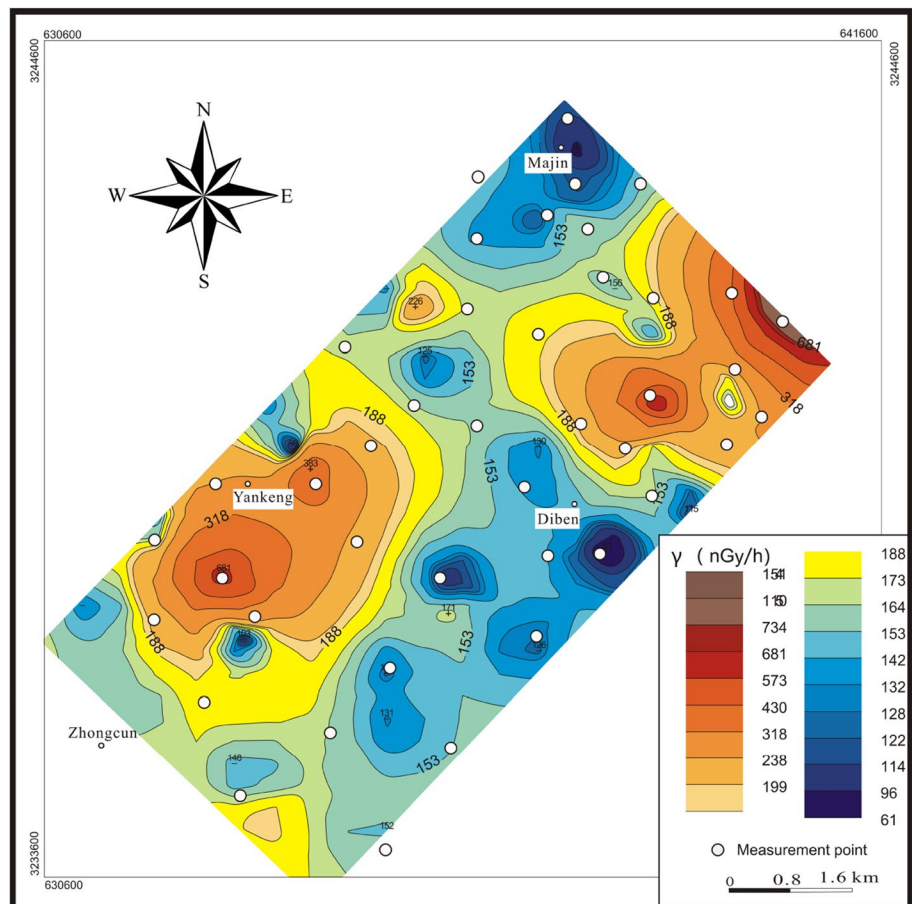
high-value centers were formed concentratively at the stone coal occurrence. The  $\gamma$ -dose rate of the high-value center in the southeast of the mining area was 738 nGy/h and that in the northwest of the mining area was 565 nGy/h. After deducting the  $\gamma$ -radiation background value (75.4 nGy/h) in the Shexian work area and the response of the instrument to cosmic rays (12.9 nGy/h), the lower limit of the  $\gamma$ -increment over the standard limit of 174 nGy/h was 262.3 nGy/h. The area of the Shexian work area with a  $\gamma$ -radiation level exceeding the limit was approximately 6.0 km<sup>2</sup>. In the concentrated distribution area of the stone coal occurrences, the effective dose caused by the  $\gamma$ -external radiation was 3.20 mSv/a, the internal radiation dose of the radon daughters was 4.98 mSv/a, and the total effective dose was 8.18 mSv/a. Compared with the field contrast points, the additional dose of the stone coal occurrences was 5.11 mSv/a.

The Kaihua work area of Zhejiang Province had an average  $\gamma$ -radiation dose rate of 205 nGy/h. This was a typical natural radiation high-background field. In the survey area, the terrestrial  $\gamma$ -radiation level was clearly unbalanced. There were many abandoned small stone coal occurrences in the northeastern margin and southwestern corner of the survey area, forming two  $\gamma$ -dose rate high-value field

centers (Fig. 3). The  $\gamma$ -dose rate in the high-value center of the mining area was 1514 nGy/h. After deducting the  $\gamma$ -radiation background value (72.3 nGy/h) in the Kaihua work area and the cosmic ray response (12.9 nGy/h), the lower limit of the  $\gamma$ -increment over the standard limit of 174 nGy/h was 259.2 nGy/h. The area of the Kaihua work area with a  $\gamma$ -radiation level exceeding the limit was more than 3.0 km<sup>2</sup>. In the center of the stone coal occurrences, the effective dose caused by the  $\gamma$ -external radiation was as high as 9.28 mSv/a, the internal radiation dose of the radon daughters was 1.70 mSv/a, and the total effective dose was 10.98 mSv/a. Compared with the field contrast points, the additional dose of the center of the stone coal occurrences was 8.45 mSv/a.

The  $\gamma$ -dose rate distribution in the coal mining area in Xiushui in Jiangxi Province was clearly controlled by the strata, and the isoline of the  $\gamma$ -radiation dose rate in the coal mining area showed an “oblique” distribution characteristic (Fig. 4). The high-value areas were concentrated in the coal seam on the north and south sides or in the carbonaceous mudstone distribution zone of the survey area, while the  $\gamma$ -radiation dose rate of the carbonate rock series in the middle was relatively low. The  $\gamma$ -dose rate in the concentrated distribution area of the stone coal occurrences was in

**Fig. 3** Isogram of the  $\gamma$ -radiation dose rate in the stone coal-bearing strata in Kaihua in Anhui Province



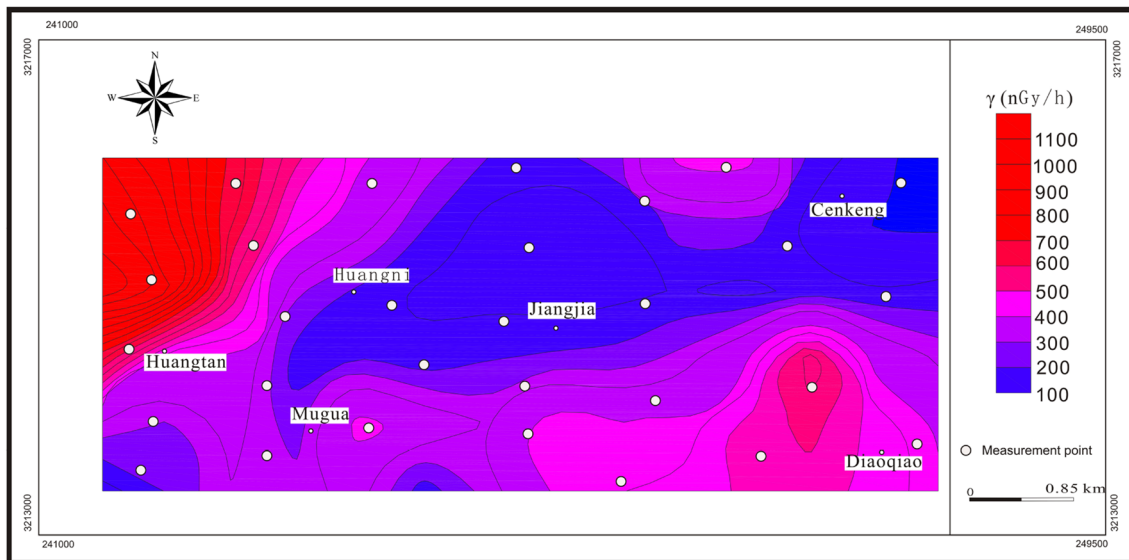


**Fig. 4** Isogram of the  $\gamma$ -radiation dose rate in the stone coal-bearing strata in Xiushui in Jiangxi Province

the range of 242–1179 nGy/h, with a mean value of up to 662 nGy/h. The mean  $\gamma$ -dose rate of the stone coal occurrences was 3.0 times that of the contrast points on the north and south sides. After deducting the  $\gamma$ -radiation field background value (143 nGy/h) in the Xiushui work area and the response of the instrument to the cosmic rays (12.9 nGy/h), the lower limit of the  $\gamma$ -increment over the standard limit of 174 nGy/h was 429.9 nGy/h. The area of the Xiushui work area with a  $\gamma$ -radiation level exceeding the limit was more than 8.0 km<sup>2</sup>. In the concentrated distribution area of stone coal occurrences, the effective dose caused by the  $\gamma$ -external radiation was 7.22 mSv/a, the internal radiation dose of the radon daughters was 2.27 mSv/a, and the total effective dose was 9.49 mSv/a. Compared with the field contrast points, the additional dose of the stone coal occurrences was 5.94 mSv/a.

## Conclusions

Previous research on the stone coal has mainly focused on the radioactivity in the solid, water and air media, while little attention has paid to the relevance of the radionuclides among different media systems. The presented study was located in major stone-coal mining areas in China with the aim to quantify the radiation. For this,  $\gamma$ -radiation measurements as well as laboratory analyses on solid, water and plant samples were presented, along with measurements of air radon concentrations. The data obtained in 5 investigated mining areas were compared with permissible radiation levels defined by Chinese national authorities, which may

reveal the radionuclide migration processes and the radiation pollution path.

1. The stone coal-bearing strata in East China are mainly in the lower Cambrian strata and distributed in a band shape along the margin of the Yangtze block, mainly in the hilly areas of Zhejiang, Jiangxi and Anhui Province. The distribution of the natural radionuclides of <sup>238</sup>U, <sup>232</sup>Th, <sup>226</sup>Ra and <sup>40</sup>K in the stone coal-bearing strata of East China shows significant spatial variability. The radionuclides of <sup>238</sup>U and <sup>226</sup>Ra are clearly enriched in the coal, coal gangue, and soil of the coal mining area.
2. The absorbed dose caused by the  $\gamma$ -external irradiation in the typical coal mining area in East China exceeded 1 mSv/a, the total effective dose exceeded 2 mSv/a, and the total effective dose of radiation to the residents in the mining area was 2.77–5.86 mSv/a. The effective doses caused by the concentration of  $\gamma$ -external irradiation in the areas of the coal mines in Shitai in Anhui, Kaihua in Zhejiang, and Xiushui in Jiangxi exceeded 5 mSv/a, and the annual effective dose of the terrestrial inhaled radon daughters in the coal mining areas of Shexian and Shitai in Anhui exceeded 3 mSv/a. The additional doses derived from the  $\gamma$ -external radiation and inhaled radon daughters in the concentrated distribution areas of the stone coal occurrences in Shexian in Anhui, Kaihua in Zhejiang and Xiushui in Jiangxi were 5.11, 8.45, and 5.94 mSv/a, respectively.
3. The exploitation and utilization of the coal-bearing formations in East China, along with the emission of the radionuclides to the air, soil and water environments, have increased the background value of the radionu-

clides in the mining areas, and sporadic radioactive contamination has occurred to the groundwater, building materials, plants and other media in the coal mining areas. The radiation dose exposed to the public in the coal mining areas has increased significantly, and there is a potential risk of radioactive contamination to the environment. Thus, monitoring of the radioactive environment in the coal mining area should be strengthened.

**Acknowledgements** This work was funded by grants of the Natural Science Foundation of Jiangsu Province (BK20151093) and the Chinese Project of the National Geological Survey (DD20160135).

## References

- Chatupnik S, Wysocka M, Janson E, Chmielewska I, Wiesner M (2017) Long term changes in the concentration of radium in discharge waters of coal mines and Upper Silesian rivers. *J Environ Radioact* 177:117–123
- China Geological Survey (2014) Quality assurance specification for laboratory of radioactive mineral analysis and testing. China Geological Survey, Beijing
- CNIC (China Nuclear Industry Corporation) (1995) Evaluation requirements for the environmental impact of uranium geological radiation environment. CNIC, Beijing
- Dai SF, Yang JY, Ward CR, Hower JC, O'Keefe JMK (2015) Geochemical and mineralogical evidence for a coal-hosted uranium deposit in the Yili Basin, Xinjiang, northwestern China. *Ore Geol Rev* 70:1–30
- Galhardi JA, Garcíatenorio R, Bonotto DM, DãAz FI, Mottaet JG (2017) Natural radionuclides in plants, soils and sediments affected by U-rich coal mining activities in Brazil. *J Environ Radioact* 177:37–47
- Huang WH, Tan XW (2002) Uranium, Thorium and other radionuclides in coal of China. *Coal Geol China* 14:55–63
- IAEA (International Atomic Energy Agency) (2014) Radiation protection and safety of radiation sources: international basic safety standards. International Atomic Energy Agency, Austria, Vienna
- Ishak AK, Dunlop AC (1985) Drainage sampling for uranium in the Torrington district, New South Wales, Australia. *J Geochem Explor* 24(1):103–119
- Jiang RR (2007) Survey of radioactive level and radiation dose to the miner in Zhejiang bone-coal mine. *Radiat Prot* 27(3):163–170,187
- Křibek B, Sracek O, Mihaljevič M, Knésl L, Majer V (2018) Geochemistry and environmental impact of neutral drainage from an uraniumiferous coal waste heap. *J Geochem Explor*. <https://doi.org/10.1016/j.gexplo.2018.05.001>. 2018
- Liu FD, Liao HT, Wang CH, Chen L, Liu SL (2006) Database of nuclide content of coal and gangue in Chinese coal mines. *Radiat Prot* 26(6):362–366
- Liu FD, Pan ZQ, Liu SL, Chen L, Wang CH, Liao HT, Wu YH, Wang NP (2007) Investigation and analysis of the content of natural radionuclides at coal mines in China. *Radiat Prot* 27(3):171–180
- Lu HJ (2003) Radioactive pollution in bone coal mining areas in western Zhejiang. *Geol Bull China* 22(9):725–728
- Luo GZ, Huang JZ, He ZY (1995) Natural radioactivity level in China. China Atomic Energy Publishing House, Beijing, pp 1–714
- Pan ZQ, Liu YY (2011) Enhanced natural radiation exposure enhanced by human activity—the largest contributor to the Chinese population dose. *Radiat Prot* 31(6):323–327
- SEPA (State Environmental Protection Agency) (1993) Specification for measurement of dose rate of ambient ground gamma radiation. SEPA, Beijing
- Skoko B, Marović G, Babić D, Šoštarić M, Jukić M (2017) Plant uptake of  $^{238}\text{U}$ ,  $^{235}\text{U}$ ,  $^{232}\text{Th}$ ,  $^{226}\text{Ra}$ ,  $^{210}\text{Pb}$  and  $^{40}\text{K}$  from a coal ash and slag disposal site and control soil under field conditions: a preliminary study. *J Environ Radioact* 172:113–121
- UNSCEAR (United National Scientific Committee on the Effects of Atomic Radiation) (2000) Sources and effects of ionizing radiation, volume 1, annex B: exposures from natural radiation sources. UNSCEAR, New York
- Wang CH, Pan ZQ, Liu SL, Yang ML, Shang B (2014) Investigation on indoor radon levels in some parts of China. *Radiat Prot* 34(2):65–73
- Wang GK, Xi CZ, Liu KK, Li YT (2017a) Assessment of coal-bearing strata uranium mineralization and impact on environment in Guizhou Province. *Coal Geol China* 29(3):58–61
- Wang HH, Zhang LX, Xu NZ, Wei XX, Dou XP (2017b) Investigation and evaluation of radioactive environment in a bone coal mine area in Xiushui County, Jiangxi Province. *Radiat Prot* 37(6):476–482
- WGSR (The Writing Group for the Summary Report on Nationwide Survey of Environmental Radioactivity Level in China) (1992) Investigation of natural radionuclide contents in soil in China. *Radiat Prot* 12(2):122–142
- WHO (World Health Organization) (2011) Guidelines for drinking-water quality, 4th edn. The World Health Organization, Geneva
- Wufuer R, Song W, Zhang D, Pan XL, Gadd G/M (2018) A survey of uranium levels in urine and hair of people living in a coal mining area in Yili, Xinjiang, China. *J Environ Radioact* 189:186–174
- Xiong ZW, Yu YL, You M, Guo CL, Zhou SK, Yu ZX (2007) Analysis of environment contamination from concomitant radioactivity of coal mine source. *J China Coal Soc* 32(7):762–766
- Ye JD, Kong LL, Li Y, Zhang L, Jiang S, Wan M, Liu HS, Zhu JQ, Shi JH, Chen CH, Zhang ZG (2004a) Study of radioactivity effect of mining and utilizing bone-coal mine on environment. *Radiat Prot* 24(1):1–23
- Ye JD, Zhu L, Wu ZM (2004b) Natural radioactivity level in bone-coal mines in Zhejiang province. *Radiat Prot Bull* 24(4):21–24
- Yue YM, Song G, Zhang ZQ, Fu YJ, Chen DY (2011) Studies on natural radioactivity of soil in North of Guangzhou. *China Environ Sci* 31(4):657–661
- Zhang ZQ, Chen DY, Zhu G, Yue YM (2011) Uptake of radionuclides from soil to plant and the discovery of  $^{226}\text{Ra}$ ,  $^{232}\text{Th}$  hyperaccumulator. *Chin J Environ Sci* 32(4):1159–1163
- Zhang KX, Pan G, He W, Xiao Q, Xu Y (2015) New division of tectonic-strata super region in China. *Earth Sci* 40(2):206–233